

# Growth and magnetic properties of Fe films epitaxially grown on Pd/Cu(001) by pulsed laser deposition

Y. Lu

Max-Planck-Institut für Mikrostrukturphysik, Weinberg 2, D-06120 Halle, Germany and Northwest Institute for Nonferrous Metal Research, P.O. Box 51, Xi'an, Shaanxi 710016, China

M. Przybylski<sup>a)</sup>

Max-Planck-Institut für Mikrostrukturphysik, Weinberg 2, D-06120 Halle, Germany and Solid State Physics Department, Faculty of Physics and Applied Computer Science, AGH University of Science and Technology, al. Mickiewicza 30, 30-059 Krakow, Poland

W. H. Wang,<sup>b)</sup> L. Yan,<sup>c)</sup> Y. Shi, J. Barthel, and J. Kirschner

Max-Planck-Institut für Mikrostrukturphysik, Weinberg 2, D-06120 Halle, Germany

(Received 29 November 2006; accepted 9 March 2007; published online 16 May 2007)

We have grown Fe films on an epitaxial Pd monolayer on Cu(001) single crystals at room temperature, both Fe and Pd by pulsed laser deposition. The presence of the Pd interlayer influences growth, structure, and magnetism of the Fe films. Up to the thickness of 1.6 ML the Fe films show an out-of-plane easy axis of magnetization which changes to in-plane above. A linear dependence of the longitudinal Kerr rotation on the Fe thickness is obtained despite existing structural transformations. A strong increase of the Curie temperature  $T_C$  is observed for the Fe films on Pd/Cu(001) compared to the Fe films grown directly on Cu(001). A correlation of the magnetic properties with possible structural changes and the role of Pd monolayer is discussed. © 2007 American Institute of Physics. [DOI: [10.1063/1.2729452](https://doi.org/10.1063/1.2729452)]

## I. INTRODUCTION

During the last decades much attention has been paid to the Fe/Cu(001) system due to its complexity of structure and magnetism. Much effort has been made to obtain the  $\gamma$ -Fe phase and clarify its magnetic properties. Bulk  $\gamma$ -Fe is stable only above 1200 K; however, it is found to be nonferromagnetic. An important route to stabilizing the  $\gamma$ -Fe phase at room temperature is to grow Fe films on appropriate substrates and under optimal preparation conditions. The Cu(001) substrate and the thermal deposition (TD) are a typical choice.

Fe ultrathin films grown on Cu(001) at room temperature by TD have been intensively studied in the past years.<sup>1-7</sup> The TD-Fe/Cu(001) films have shown a complex structural transformation with increasing Fe film thickness from 2 ML to above 11 ML. Low-energy electron diffraction (LEED) measurements have indicated that, up to 4 ML, TD-Fe/Cu(001) films possess a face-centered tetragonal (fct) structure with an  $n \times 1$  reconstruction due to sinusoidal shifts and vertical buckling of the atoms ( $n=4,5$ ).<sup>1-4</sup> Between 5 and 11 ML, only the top two layers still have tetragonal expansion,<sup>1</sup> whereas the inner layers become an isotropic fcc phase. Around 11 ML the fcc-bcc structural phase transition occurs. The observed ferromagnetic order in 2–4 ML thick films is usually attributed to the existence of the fct structure.<sup>1-3</sup> The

drop of saturation magnetization observed for TD-Fe/Cu(001) films in the thickness range between 5 and 11 ML is often attributed to a nonmagnetic or antiferromagnetic state of the inner layers which is related to their fcc structure.<sup>1-3,6</sup> Recent investigations by scanning tunneling microscopy (STM) on ultrathin Fe films on Cu(001), however, suggest bcc-like  $n \times 1$  phases existing below 5 ML film thickness, which could offer a straightforward explanation for the ferromagnetic properties observed in this thickness range.<sup>8</sup> However, it is also reported that this kind of the surface reconstruction could result from the hydrogen adsorption at low temperature.<sup>9</sup> Finally, the relationship between structure and magnetism of TD Fe/Cu(001) films is still under discussion.

The application of the pulsed laser deposition (PLD) method for growing Fe/Cu(001) films at room temperature has greatly influenced the structure and magnetism.<sup>10-12</sup> A layer-by-layer growth mode of Fe/Cu(001) from the initial stages has been obtained, which was confirmed by reflection high-energy electron diffraction (RHEED) and STM.<sup>11</sup> An important finding is a nearly ideal strained fcc structure without reconstructions at all thickness below 10 ML of Fe.<sup>10,11</sup> However, this seemingly simple structure has displayed more complicated magnetic properties.<sup>10-12</sup> Up to 2 ML the PLD-Fe films have a perpendicular easy magnetization axis. A spin reorientation transition (SRT) occurs at about 2 ML, switching the magnetization in-plane. Between 5 and 7 ML the Fe films undergo a second SRT from in-plane to perpendicular. The third SRT is completed above 10 ML of Fe, again with the in-plane magnetization for the bcc phase. The thickness dependence of the saturation magnetization indicates that below 4 ML the PLD-Fe films have a high mag-

<sup>a)</sup>Electronic mail: [mprzybyl@mpi-halle.mpg.de](mailto:mprzybyl@mpi-halle.mpg.de)

<sup>b)</sup>Present address: Nanotechnology Research Institute, National Institute of Advanced Industrial Science and Technology (AIST), 1-1-1 Umezono, Tsukuba, Ibaraki 305-8568, Japan.

<sup>c)</sup>Present address: Shanghai Institute of Technical Physics, Chinese Academy of Sciences, Shanghai 200083, China.

netic moment, as is found for the TD-Fe films.<sup>10–12</sup> Above 4 ML, however, the saturation magnetization drops almost monotonically except for a small plateau region during the second SRT between 5 and 7 ML. This decrease of magnetization has been explained as a result of increasing nonferromagnetic bulklike fcc phase due to the local strain relaxations.<sup>10,11</sup> It is difficult to give a reasonable explanation of the SRT behavior in the PLD Fe/Cu(001) films and to correlate it with the film structure.

It is known that surface and interface effects could be important for the magnetic properties of the ultrathin Fe films. Our current work is focused on the influence of a Pd interlayer on the structure and magnetic properties of PLD-grown Fe films on Cu(001). In this study we have used PLD to grow epitaxially 1 ML of Pd on Cu(001) substrate. During the single monolayer Pd deposition by PLD the ordered Cu(001)*c*(2×2)-Pd surface alloy, which was usually observed for thermally deposited Pd films,<sup>13</sup> could be avoided due to very high nucleation density. It has been shown by surface x-ray diffraction experiments that, for 1.1 ML of PLD-grown Pd on Cu(001), more than 90 % of the deposited Pd is concentrated in the topmost layer, i.e., almost the whole surface of Cu is covered by Pd atoms.<sup>14</sup> The growth of Pd is pseudomorphic to the Cu(001) substrate. Therefore, subsequently PLD-deposited Fe layers have the same lattice mismatch with the Pd interlayer as at the Fe/Cu(001) interface. Nevertheless, structural and magnetic properties of the PLD-Fe/Pd/Cu(001) system demonstrate a variety of features which are attributed to the Fe/Pd interface.

## II. EXPERIMENT

The films were grown by PLD in a multichamber ultra-high vacuum system with a base pressure  $<5 \times 10^{-11}$  mbar and less than  $<2 \times 10^{-10}$  mbar during deposition. Prior to deposition the copper substrate was cleaned by cycles of Ar<sup>+</sup> sputtering followed by annealing at 900 K until only Cu Auger electron spectroscopy (AES) spectra, sharp low-energy electron diffraction LEED spots, and atomically smooth terraces under STM were observed. The substrate temperature was kept at room temperature during deposition. The substrate was placed about 100–130 mm away from Pd target. The pulse laser energy was set to 325 mJ (34 ns pulse length, repetition rate 10 Hz). After deposition of Pd the target was changed to Fe for further laser ablation. The whole growth process of films was monitored by RHEED. All STM measurements were performed in the constant current mode at 0.2–0.5 V positive tip bias voltage and 0.1–0.5 nA tunneling current. The crystalline structure of the films was evaluated based on a kinematic analysis of the LEED *I*(*E*) curves for the (00) diffraction beam.<sup>5</sup> The magnetic properties were recorded by longitudinal and polar magneto-optical Kerr effect (MOKE), where a *p*-polarized laser beam with a wavelength of 675 nm (photon energy 1.84 eV) was used. For the longitudinal MOKE, the incidence angle (with respect to the surface normal) of the probing laser beam was  $68^\circ \pm 2^\circ$ . For the polar MOKE, the incidence angle was approximately  $5^\circ$  (nearly normal incidence).

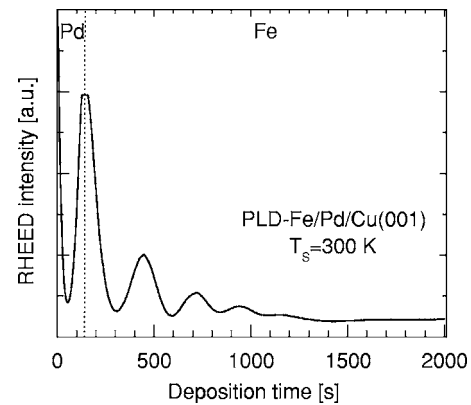


FIG. 1. RHEED specular beam intensity oscillations vs time during deposition of Fe and Pd on Cu(001) at room temperature. The Pd layer thickness of 1 ML was quantified by STM and AES.

## III. RESULTS

### A. Structural properties

Figure 1 shows the RHEED intensity of the specular beam versus time during the deposition of Pd and Fe on Cu(001) at room temperature. The first Pd monolayer is completed and also the Cu substrate is fully wetted as the first RHEED intensity oscillation is finished. The growth of subsequent Fe layers proceeds in the layer-by-layer mode until about 4 ML. We have not observed RHEED intensity oscillations beyond this point because of increasing surface roughness. The surface roughening is directly linked with the structural transition discussed later. For PLD-Fe films directly deposited onto Cu(001), i.e., without the Pd interlayer, eight RHEED intensity oscillations are visible.<sup>11</sup> This difference in RHEED intensity behavior implies a dissimilarity in the morphology and structure between the PLD-Fe/1MLPd/Cu(001) and PLD-Fe/Cu(001) systems.

*I*-*V* LEED studies were undertaken to investigate the structural properties of PLD-grown Fe/Pd/Cu(001) films and further to give a comparison with the PLD-Fe/Cu(001) system. LEED *I*(*E*) curves for the (00) diffraction beam were taken at an angle of incidence of about  $6^\circ$  to the surface normal at room temperature. They are shown in Fig. 2. We first discuss the *I*(*E*) curve for PLD-grown 1 ML Pd on Cu(001) substrate. We have obtained one sequence of sharp peak maxima with a rather obvious energy shift toward the lower-energy direction in comparison with that from Cu(001) substrate. This means a larger vertical interlayer distance. Upon deposition of Fe layers by PLD up to 4 ML, LEED *I*(*E*) curves exhibit only one family of characteristic peaks with a nearly constant shift of energy peaks. Therefore, we believe that PLD-grown Fe/Pd/Cu(001) films have a distorted fcc structure (fct) up to a thickness of 4 ML. The peak sequence of the fct phase is marked by dashed lines in Fig. 2. With further increasing Fe film thickness above 4 ML, the energy positions of the maxima gradually shift toward higher energies and at a thickness of 6.5 ML reach the positions corresponding to the Cu(001) substrate. This might indicate a fcc structure of the whole Fe/Pd/Cu stack. The structural transition from fct to fcc occurs over a narrow film thickness range of about 2 ML above 6 ML Fe. Moreover, the fcc

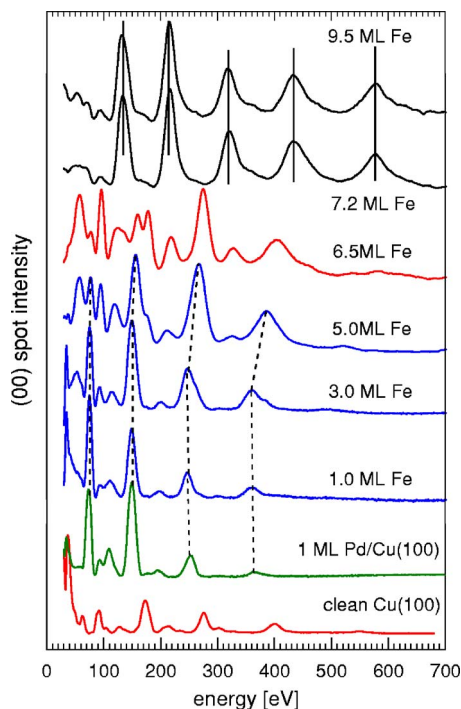


FIG. 2. (Color online) Intensity vs energy curves of the LEED (00) spot for the clean Cu(001), 1 ML Pd on Cu(001), and PLD Fe films on 1 ML Pd/Cu(001) measured at room temperature. The Fe thickness is indicated on the right-hand side. The kinematic maxima related to the fct-like and bcc structures are marked by dashed and solid lines, respectively.

peaks disappear above the thickness of 7 ML, whereas another peak sequence (marked by solid lines in Fig. 2) appears in the LEED  $I(E)$  curves. Actually, this peak sequence becomes visible as the Fe film thickness just exceeds 4 ML. The energetic positions of these peaks remain unchanged until 9.5 ML, i.e., up to the thickest film which we investigated. The peak sequence is identified as the bcc structure of Fe. Such a structural transition from fct via fcc (within only about 2 ML thickness) to bcc is very different from that in the PLD Fe/Cu(001) films, where the Fe films remain in fcc structure below 10 ML.<sup>10,11</sup>

In Fig. 3 the average interlayer spacing is depicted as a

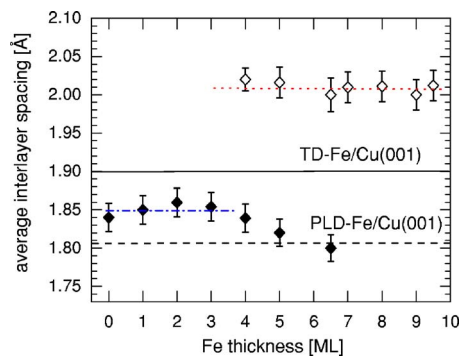


FIG. 3. (Color online) Thickness dependence of the vertical interlayer distances  $a_{\perp}$  for the Fe films on 1 ML Pd/Cu(001). The values of  $a_{\perp}$  were calculated within the kinematic approximation from the  $I(E)$  curves in Fig. 2. The dotted and dash-dotted lines are guide to the eyes giving the bcc and fct interlayer spacings, respectively. The solid line shows the value for TD-Fe/Cu(001) and the dashed line for PLD-Fe/Cu(001) obtained in the Fe thickness range up to 3 ML.

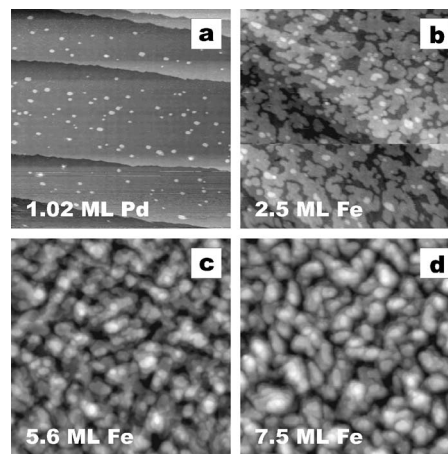


FIG. 4. STM images for (a) 1.02 ML PLD-grown Pd on Cu(001) substrate; (b) 2.5 ML Fe on 1 ML Pd/Cu(001); (c) 5.6 ML Fe on 1 ML Pd/Cu(001); (d) 7.5 ML Fe on 1 ML Pd/Cu(001). The size of STM images is  $100 \times 100 \text{ nm}^2$ . Some ridgelike structures are visible already for 5.6 ML thick Fe film on 1 ML Pd/Cu(001).

function of the Fe film thickness. These values of  $a_{\perp}$  were extracted within the kinematic approximation based on the measured  $I(E)$  curves shown in Fig. 2.<sup>5</sup> At low coverage, i.e., below 4 ML, the vertical interlayer distance is roughly constant,  $a_{\perp} = 1.85 \text{ \AA}$ .  $a_{\perp}$  then gradually decreases to  $1.80 \text{ \AA}$  at 6.5 ML. Above 4 ML for the bcc phase the interlayer distance  $a_{\perp}$  jumps to  $2.01 \text{ \AA}$ . This value agrees well with that of the Fe bcc(110)-like structure ( $a_{\perp} = 2.02 \text{ \AA}$ ). In the thickness range between 4 and 6.5 ML both phases, fct-like Fe and bcc-like Fe, coexist.

In order to get more information about the structural transformation going on in the thickness range between 4 and 6.5 ML, STM experiments have been performed. Figure 4(a) displays a STM image of PLD-grown Pd film of a thickness of 1.02 ML on Cu(001) substrate. A fully wetting substrate surface, together with a few small islands in the second monolayer, is observed. This is characteristic of an ideal layer-by-layer growth mode. The morphology of the Cu substrate is not changed upon Pd deposition. Upon deposition of Fe layers on the Pd buffer monolayer, the surface morphology exhibits a pronounced evolution, which reflects the change of the growth mode and structural transformation of PLD-Fe films. Here, we give the representative STM images for three different film thickness regions. In Fig. 4(b) the STM image for 2.5 ML Fe on 1 ML Pd/Cu(001) is displayed. We have observed three gray levels. This is a typical surface morphology for the Fe film with a thickness below 4 ML. In this thickness region, the layer-by-layer growth mode and the pure fct phase are found from the RHEED and  $I$ - $V$  LEED studies reported above. The smooth film surface, therefore, should be expected up to about 4 ML. In the structural transformation region above 4 ML, an increase in the surface roughness was detected, as shown in Fig. 4(c) for 5.6 ML of Fe on 1 ML Pd/Cu(001). These island structures are attributed to a formation of the bcc precipitates, which are typically oriented along the  $\langle 011 \rangle$  directions of the Cu(001) substrate.<sup>15</sup> The  $I$ - $V$  LEED data shown in Figs. 2 and 3 have confirmed this point. When the Fe film thickness exceeds 6.5 ML, the STM image, for e.g., 7.5 ML Fe on 1 ML Pd/

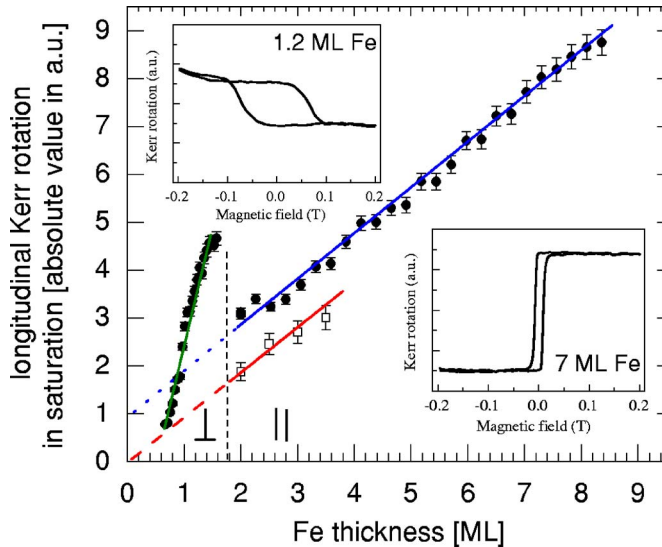


FIG. 5. (Color online) Thickness dependence of the longitudinal Kerr rotation measured along the  $[100]$  direction of Cu substrate at 60 K for Fe/1 ML Pd/Cu(001) films (solid circles). Two representative MOKE loops for 1.2 and 7 ML of Fe are shown in the insets. The saturation Kerr rotation from the reference sample of PLD-Fe/Cu(001) for a thickness range between 2 and 4 ML (in which the easy magnetization axis lies in the film plane), is indicated by the open square symbols.

Cu(001) [Fig. 4(d)], indicates a fully bcc transformed structure. This agrees well with the results from the  $I$ - $V$  LEED measurements suggesting a pure bcc phase for the Fe films thicker than 6.5 ML.

We can conclude that the transformation to the bcc structure persisting already at the thickness of 4.0 ML is a main reason of the disappearing RHEED intensity oscillations at this thickness. This kind of structural transition enhances the surface roughness in the usual sense as it was observed for the TD Fe/Cu(001) system<sup>2</sup> above 10 ML Fe. The structural transformation occurs within a very narrow thickness range. We suggest that single monolayer of Pd exerts a significant influence on the growth and structure of Fe films. This kind of structural difference will result in different magnetic properties.

## B. Magnetic properties

Detailed MOKE measurements were performed at 60 K in both longitudinal and polar geometries for various Fe coverage. Above about 2 ML we have not detected polar hysteresis loops, even at a magnetic field of 0.8 T, showing that the PLD-grown Fe/Pd/Cu(001) films have in-plane magnetic anisotropy in this thickness range. There exists no spin reorientation transition for the Fe/Pd/Cu(001) films in the thickness between 5 and 7 ML as it was observed for the Fe films grown by PLD directly on Cu(001). Figure 5 displays the Fe thickness dependence of saturation Kerr rotation in the longitudinal geometry measured at 60 K, where the magnetic field was applied along the  $[100]$  direction of the Cu(001) substrate. In the inset of Fig. 5 two representative hysteresis loops for 1.2 and 7 ML are plotted. For thinner films, i.e., below 1.6 ML of Fe on Pd/Cu(001), the signal is much higher than that what would result from the extrapolation of the thickness dependence of the Kerr rotation measured for

thicker Fe films grown by PLD directly on Cu(001). Moreover, the loops are of very large coercivity and reversed, i.e., a negative Kerr rotation is measured in saturation for a positive field. Finally, such loops disappear in a very narrow thickness range just below 1.6 ML. This seemingly unusual behavior is caused by a slight misalignment of the sample plane from the direction of the large external magnetic field. In such a geometry, the field component perpendicular to the sample plane is introduced, which can be sufficient to magnetize the sample. In the case where the polar signal would appear, it could be “projected” to the longitudinal MOKE geometry. Consequently, in the case of PLD-Fe/1 ML Pd/Cu(001), the abnormal longitudinal Kerr signal below 1.6 ML is actually the polar signal detected due to the effective perpendicular anisotropy of the system in this thickness range. These results (Fig. 5) can be easily misinterpreted when the sample misalignment is not noticed.

The PLD-Fe/Pd/Cu(001) films display different magnetization as a function of thickness compared to the PLD-Fe/Cu(001) films, in particular above 4 ML of Fe. In both cases, below roughly 2 ML of Fe, the films exhibit perpendicular magnetization. Below 4 ML a linearly dependent saturation Kerr intensity measured in longitudinal geometry is discovered for the PLD-Fe/Cu(001) films, suggesting a high-spin state.<sup>12</sup> We have repeated the MOKE experiments for the PLD-Fe/Cu(001) system. In Fig. 5 we show the longitudinal Kerr measurement result only for a film thickness between 2 and 4 ML. Then, it is possible to directly compare the magnetic properties of two different systems. We have found that for the PLD-Fe/Pd/Cu(001) films with a thickness of 2–4 ML Fe, the slope of the Kerr rotation as a function of the film thickness is the same as for the PLD-Fe/Cu(001) films. This implies a high-spin state also in the PLD-Fe/Pd/Cu(001) films between 2 and 4 ML Fe. Above 4 ML the Fe/Pd/Cu(001) films keep the high-spin state also in the structural transformation regime, whereas the Fe/Cu(001) films have a nonuniform spin phase manifesting itself in an almost monotonic drop of the Kerr rotation.<sup>12</sup> Additionally, the PLD-Fe/1 ML Pd/Cu(001) system shows an obvious positive offset of the saturation Kerr rotation, if one extrapolates the thickness dependence of the saturated Kerr rotation above 2 ML back to zero thickness of Fe. This suggests an additional contribution of the Fe/Pd interface to the total Kerr rotation of PLD-Fe/1 ML Pd/Cu(001) system.<sup>16</sup>

In order to get some insight into the exchange interaction in the PLD-Fe/Cu(001) and PLD-Fe/Pd/Cu(001) systems of varying structure, we performed measurements of Curie temperature. The thickness dependence of the Curie temperature is plotted for the Fe/Pd/Cu(001) films in Fig. 6. The temperature evolution of the longitudinal Kerr rotation loops was measured to determine  $T_C$ . For thicker films the Curie temperature was obtained by extrapolating the Kerr rotation behavior from the phenomenological power-law fits to the data measured below 525 K. We have found that the  $T_C$  versus thickness data roughly follow a monotonic curve with a plateau below 5 ML. We have observed a rapid change in the  $T_C$  values in the submonolayer and monolayer region, and a more gradual change for the thicker films. This behavior is very different from that found for the PLD-Fe/Cu(001) films

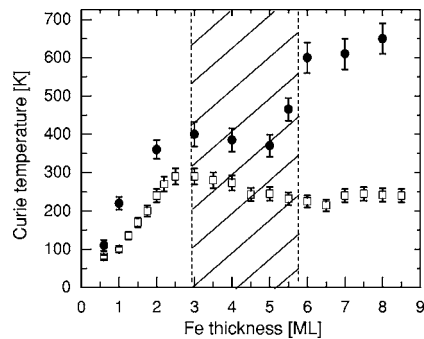


FIG. 6. The Curie temperature vs Fe thickness for PLD-Fe/Pd/Cu(001) (as indicated by solid circle symbols). The maximal measurement temperature in our MOKE setup was 525 K. The  $T_C$  for the Fe coverage above 5 ML was extrapolated by the temperature dependence of magnetization based on a power-law behavior. The  $T_C$  data of the PLD-Fe/Cu(001) system (square symbols) are from Refs. 11 and 12. A thickness range of the expected structural phase transition for PLD-Fe/Pd/Cu(001) is additionally marked.

and also for TD-Fe/Cu(001) films. In particular, for the PLD-Fe/Cu(001) films, a monotonic increase of  $T_C$  with increasing film thickness was detected only below 2 ML, while the maximum  $T_C$  of about 290 K at 3 ML and the approximately constant  $T_C$  with a dip of 210 K at 6.5 ML was found (see Fig. 6).<sup>12</sup> It should be pointed out that the  $T_C$  values for PLD-Fe/Pd/Cu(001) are higher than those for PLD-Fe/Cu(001) in the investigated thickness range.

#### IV. DISCUSSION

Compared to the PLD-Fe/Cu(001) system, the PLD-Fe/Pd/Cu(001) system has displayed different structural properties characterized by the fct-to-bcc phase transition at relatively low thickness and at the same time a different magnetic behavior. We first discuss the structure of the Fe/Pd interface. The pseudomorphic Pd interlayer grown on Cu(001) has the same in-plane lattice constant as the Cu(001) substrate. The shift of the energy positions of the maxima in the  $I(E)$  LEED curve for 1 ML Pd on Cu(001) toward lower energies suggests a larger interlayer lattice spacing. For the Fe overlayer, therefore, the actual lattice mismatch with the Pd interlayer is almost the same as at the Fe/Cu(001) interface. In the case of Fe/1 ML Pd/Cu(001), we deal with an only slightly mismatched Fe/Pd interface. But, this is not the only reason why the Fe/Pd interfaces in the Fe/1 ML Pd/Cu(001) and in the Fe/Pd(001) system are different. Also, the Fe/Pd intermixing in both cases might not be the same; however, in both cases it is expected to occur if we consider that the PLD technique was chosen for the deposition of Fe.

Upon depositing PLD Fe up to 4 ML on the 1 ML Pd/Cu(001) surface, we have obtained a uniformly tetragonally distorted fcc structure with an approximate atomic layer distance  $d_{\perp} = 1.85 \text{ \AA}$ . This value is smaller than that of TD-Fe/Cu(001) films ( $d_{\perp} = 1.90 \text{ \AA}$ ) but larger than that of PLD-Fe/Cu(001) films ( $d_{\perp} = 1.81 \text{ \AA}$ ) in the similar thickness region.<sup>5,11</sup> For TD-Fe/Cu(001) films, in fact, the fct phase with  $d_{\perp} = 1.85 \text{ \AA}$  was detected in the thickness range between 4 and 10 ML. Moreover, by the weak tetragonal distortion in this case, only the topmost layers are affected.<sup>17</sup> Compared to

the PLD-Fe/Cu(001), the presence of the Pd interlayer enhances the tetragonal distortion. This might be due to an intermixing between Fe and Pd atoms and a formation of the Fe/Pd alloy in the interface. With increasing Fe thickness above 4 ML, the fct structure of the PLD-Fe/1 ML Pd/Cu(001) films evolves into a mixture of fcc and bcc (with a  $\langle 110 \rangle$  orientation) structures. Finally, at the thickness of 7 ML, the whole Fe film exhibits bcc structure. This fct-fcc-bcc transition process involves only a narrow 2.5 ML thickness range between 4.0 and 6.5 ML Fe coverage, i.e., the whole structural transformation is quite abrupt, whereas in the PLD-Fe/Cu(001) system there is an extended range of coexistence of fcc and bcc regions in the film (between 5.0 and 10.0 ML), followed by an abrupt transformation of the whole film to the bcc structure above 10.0 ML Fe coverage. Moreover, in real space, from STM images one can conclude that, in the case of Fe/1 ML Pd/Cu(001), the fcc and bcc island-shaped regions are of equally small size of typically 5 nm and evenly mixed throughout the whole film area, while in the pure Fe/Cu(001) system large-scale fcc areas (typically 50–100 nm size) are surrounded by quasi-one-dimensional bcc features (“precipitates” = “ridges”). The presence of the interface alloy and the structural transformation analyzed above determines the specific magnetic behavior of the Fe/1 ML Pd/Cu(001) films as compared to the well-known magnetic properties of Fe/Cu(001).

First, we consider the difference in the easy magnetization axis direction. Spin alignment and spin reorientation transitions are phenomenologically understood as the result of the competition between bulk, surface, and interface contributions to the magnetic anisotropy energy (MAE). For ultrathin fcc (or fct) Fe films the surface and/or interface anisotropy favors perpendicular magnetization. For the vertically expanded fct Fe films additionally magnetocrystalline anisotropy contributes to perpendicular anisotropy. In the thickness range where the perpendicular contributions are sufficiently strong to overcome the shape anisotropy (favoring always in-plane magnetization) the films are magnetized out of plane. For PLD-Fe/Cu(001) films a perpendicular easy magnetization below 2.0 ML has been detected,<sup>12</sup> while for TD-Fe/Cu(001) films perpendicular magnetic anisotropy (PMA) is observed over the whole fct/fcc structural range up to 10.0 ML Fe. The effect of interfacial intermixing in the process of PLD could reduce the perpendicular anisotropy in comparison to TD-deposited Fe films on Cu(001). This intermixing effect is likely to be responsible for the limited PMA range also in our case of PLD-Fe/1 ML Pd/Cu(001) films, where we observe out-of-plane magnetization only up to 1.6 ML in analogy to PLD-Fe/Cu(001). The induced magnetic moment of Pd expected in contact with a ferromagnetic metal such as Fe could contribute to the overall MAE of the system,<sup>18</sup> e.g., by increasing the shape anisotropy energy. Then, in accordance with the foregoing considerations, at increasing Fe coverage between 2.0 and 4.0 ML, both the PLD-Fe/Cu(001) and the PLD-Fe/1 ML Pd/Cu(001) films show clear in-plane anisotropy.

At their structural transition between 4.0 and 6.5 ML, the PLD-Fe/1 ML Pd/Cu(001) films preserve this in-plane anisotropy, whereas around 5.0 ML the PLD-Fe/Cu(001) undergo

a second SRT from in-plane back to out-of-plane magnetization. The reason for the second SRT in PLD-Fe/Cu(001) may be explained by the observation of a spin density wave (SDW) in TD-Fe/Cu(001) in the thickness range between 5.0 and 10.0 ML.<sup>7</sup> This has been attributed to the inner layers in the film which—in contrast to near-surface layers—are fully relaxed to fcc structure. The same SDW can be expected for PLD-Fe/Cu(001) in the same thickness range, in which identical structure as in TD-Fe/Cu(001) has been found by tensor LEED analysis.<sup>19</sup> The presence of SDW stretching over about 3–7 layers in the film, depending on the total thickness, considerably reduces the shape anisotropy energy thus favoring out-of-plane magnetization, causing the second SRT in the PLD-Fe/Cu(001) films at around 5.0 ML [on the other hand, in TD-Fe/Cu(001) the sign of the MAE does not change here because of the continuously dominating perpendicular anisotropy]. Moreover, apparently the difference in perpendicular and shape anisotropy in PLD-Fe/Cu(001) seems to be so small that coexistence of different domains becomes feasible. In contrast to PLD-Fe/Cu(001) with its relatively large (50–100 nm) flat areas of undistorted fcc Fe above 5.0 ML film thickness (apparently being the prerequisite for the occurrence of SDW), in the rough, small-size islandlike structure of mixed fcc/fct/bcc in the PLD-Fe/1 ML Pd/Cu(001) films of the same thickness, no SDW can be formed. Thus, here the proportionality between film thickness and total shape anisotropy energy is preserved. As a consequence in-plane magnetic anisotropy persists (and becomes even enforced with increasing film thickness). Small size morphology of the PLD-Fe/1 ML Pd/Cu(001) films above 4 ML seems to be related to the presence of Pd atoms dispersed in the Fe films during the PLD process, increasing the overall lattice mismatch in the system, which finally can be accommodated only by the decay of the originally smooth film (below 4.0 ML thickness) into small islands. Similar morphology is found for Fe/Pd(001) films above 4.0 ML Fe,<sup>21</sup> where also a considerable alloying of Pd into the film has been reported.<sup>22</sup> After the transition to the stable bcc-Fe structure, in all (PLD as well as TD) Fe/Cu(001) films but also in the PLD-Fe/1 ML Pd/Cu(001) system investigated here, the easy magnetic axis lies in the plane. The fact that this transition for the PLD-Fe/1 ML Pd/Cu(001) films is complete at much smaller thickness (<7.2 ML) prevents this system from undergoing any additional SRTs at larger film thickness except the one around 1.6 ML of Fe.

Now we discuss how the Kerr rotation, which is related to the film magnetization, varies with film thickness. A linear increase of Kerr rotation between 2.0 and 4.0 ML Fe is common for both PLD-Fe/Cu(001) and PLD-Fe/1 ML Pd/Cu(001) systems. In this thickness range both types of films have fct structure, though of different degrees of tetragonal distortion. The slopes of both thickness dependency curves are almost the same; thus, the magnetic moment per layer is approximately the same (taking into account that magneto-optical conditions for the growing Fe film are similar). Above about 7 ML the bcc transformed Fe obviously is characterized by the bulk magnetic moment of iron  $2.2 \mu_B$  per atom). The further linear increase of Kerr rotation with film thickness, obeying the same slope as the dependence at low

thickness, points to the conclusion that the magnetic moment of Fe in the fct range is of similar value as in the higher thickness range. Because magneto-optics is not a method suited for straightforward determination of magnetic moments, within our measurement accuracy we are unable to decide whether the magnetic moment per layer between 2.0 and 4.0 ML Fe film thickness is closer to the bulk bcc Fe moment or to the theoretical high-spin fcc Fe value. Nevertheless, the fact that the full thickness range between 2.0 and 9.0 ML for the PLD-Fe/1 ML Pd/Cu(001) system can be described by one linear dependence leads to the conclusion that the magnetic state of Fe atoms at low temperature (60 K) in this film is invariant with respect to occurring structural changes. In particular, the range between 4.0 and 6.5 ML Fe with its complex, mixed structure (see the *I-V* LEED spectra of Fig. 2) does not show up in a deviation from the linear behavior (Fig. 5, solid circles). This means that the exchange interaction is strong enough to align all the spins parallel.

The offset of the saturation Kerr rotation at zero thickness for the Fe films grown on 1 ML Pd/Cu(001) compared to films grown directly on Cu(001) clearly demonstrates the effect of the buffer-Pd on the total magneto-optical response. While for the PLD-Fe/Cu(001) films there is no offset detectable within the measurement accuracy, a positive offset is measurable for the PLD-Fe/1 ML Pd/Cu(001) system when extrapolating the linear dependence above 2 ML Fe down to zero thickness. A similar offset effect was found for the Co/1 ML Pd/Cu(001) system.<sup>20</sup> Such positive offset implies an additional contribution to the total Kerr rotation from the ferromagnet/Pd interface.<sup>23</sup> We found the Kerr rotation offset caused by the Fe/1 ML Pd interface roughly equivalent to the Kerr rotation produced by a 1.0 ML thick layer in the Fe film. This additional increase of the Kerr rotation gives indirect evidence for the Fe induced spin polarization of the Pd interlayer as well as of the increased magnetic moment in the interfacial atomic layer of Fe in the Fe/Pd interface. In the case of Fe grown on Pd(001) by either PLD or TD, an offset originating from the Fe/Pd interface could be observed as well, though its value was smaller (corresponding to 0.6 ML within the Fe film<sup>24</sup>). One might speculate why the offset in the system Fe/1 ML Pd/Cu(001) amounts to 1.0 ML Fe, while only 0.6 ML Fe in the Fe/Pd(001) system: is it due to a different level of dispersion of Pd in the Fe depending on whether the deposition occurs on bulk Pd or on a monolayer Pd film? After all, this question cannot be resolved solely by Kerr effect measurement. It is thus highly desirable to determine the absolute values of magnetic moments of Pd and Fe layer using element-specific magnetic circular dichroism in future experiments.

The PLD Fe/1 ML Pd/Cu(001) films display a monotonic thickness dependence of Curie temperature with an almost steady value in the structural transition region. According to finite size theory the Curie temperatures  $T_C(n)$  of magnetic thin films increase with increasing film thickness until  $T_C$  approaches the value for the bulk material.<sup>25</sup> The scaling law is strictly valid only if the whole film is uniformly magnetic. This is true for the PLD-Fe/1 ML Pd/Cu(001) films below 3.0 ML thickness. Many factors, such as structural changes, spin reorientation transitions, and local

nonuniformly magnetized phases, can significantly influence the thickness dependence of  $T_C$ . For PLD-Fe/Cu(001) films only below 2 ML, the  $T_C(n)$  behavior can be explained by the law, although it has been believed that the Fe films are in the high-moment state below 4 ML.<sup>10,11</sup> For PLD-Fe/Cu(001) system, the abrupt increase of  $T_C$  to the temperatures higher than 450 K occurs when the fcc-to-bcc phase transition is completed at the Fe thickness of more than 10 ML (not shown in Fig. 6).<sup>11</sup> A similar situation was found in the TD-Fe/Cu(001) system. The strong suppression of  $T_C$  between 3.0 and 10.0 ML seems to be related to the remaining 2 or 3 near surface “live” ferromagnetic layers, while the rest of the film near 300 K is nonmagnetic. At temperatures above 160 K also the spin density wave feature no longer persists. This holds for both PLD- and TD-Fe/Cu(001) systems.

For the PLD-Fe/1 ML Pd/Cu(001) system, in the thickness range from 3.0 ML Fe up to the thickness where the bcc transformation is complete, it seems that not the whole film participates equivalently to the ferromagnetic order at temperatures near 400 K. However, we cannot say that, analogously to Fe/Cu(001) system, only 2 or 3 layers are participating in long-range ferromagnetic order, because this is not seen from the monotonically increasing Kerr signal with increasing thickness measured at low temperature (Fig. 5). Nevertheless, most likely—as for Fe/Cu(001)—the part of the film which is structurally relaxed to fcc becomes nonmagnetic earlier upon temperature increase in comparison to that part of the film which is of fct (and bcc) structure. In this case only that part of the film which still keeps the fct structure contributes to the ferromagnetic order at temperatures near 400 K. In other words, the temperature dependence of magnetization is not homogeneous over the whole film, thus producing a nonincreasing  $T_C$  in the thickness range between 3 and 5 ML. In Fig. 6 we clearly see that at the same thickness  $T_C$  is higher for the PLD-Fe films grown on 1 ML Pd/Cu(001) in comparison to those grown directly on Cu(001). The enhancement of  $T_C$  in the case of Fe/1 ML Pd/Cu(001) can be explained as the result of the induced magnetic moment in the Pd-interlayer plus the additional magnetic moment of the Fe at the Pd interface which enhances the magnetic coupling in the whole film leading to considerably larger  $T_C$  values. Our result agrees qualitatively with the theoretical calculations done by Strandburg *et al.*, where they analyzed the effect of Fe-Pd coupling on the  $T_C$  behavior for the system of Fe grown on Pd(001).<sup>26</sup> A more pronounced enhancement of the  $T_C$  for Fe/1 ML Pd/Cu(001) in comparison to Fe/Cu(001) is observed above the Fe thickness of 6 ML. This is clearly related to the bcc structure of Fe which is finally developed in this thickness range.

## V. CONCLUSION

We have investigated the structural and magnetic properties of Fe/1 ML Pd/Cu(001) films grown by pulsed laser deposition. Structure analysis has shown that below 4 ML the Fe films have a fct lattice structure with an interlayer

distance of 1.85 Å. The fct-fcc-bcc structural transformation occurs between 4 and 6.5 ML. The uniformly magnetized phase of the Fe films above 2 ML has been confirmed by MOKE measurements, which are independent of the structural transition. Similarly to the PLD-Fe grown on Cu(001), a perpendicular easy axis of magnetization in the PLD-Fe/Pd/Cu(001) was found below the thickness of 1.6 ML. An enhanced magneto-optical response was found which is related to the spin polarization of the Pd interlayer. An increased Curie temperature of the Fe/Pd/Cu(001) system in comparison to that of Fe/Cu(001) is explained by polarized Pd at low thickness and by the development of bcc-Fe above the thickness of 6 ML.

## ACKNOWLEDGMENTS

The authors are grateful to H. Menge and G. Kröder for their excellent technical assistance and support.

- <sup>1</sup>J. Thomassen, F. May, B. Feldmann, M. Wuttig, and H. Ibach, *Phys. Rev. Lett.* **69**, 3831 (1992).
- <sup>2</sup>D. Li, M. Freitag, J. Pearson, Z. Q. Qiu, and S. D. Bader, *Phys. Rev. Lett.* **72**, 3112 (1994).
- <sup>3</sup>S. Müller, P. Bayer, C. Reischl, K. Heinz, B. Feldmann, H. Zillgen, and M. Wuttig, *Phys. Rev. Lett.* **74**, 765 (1995).
- <sup>4</sup>K. Heinz, S. Müller, and P. Bayer, *Surf. Sci.* **352–354**, 942 (1996).
- <sup>5</sup>M. Zharnikov, A. Dittschar, W. Kuch, C. M. Schneider, and J. Kirschner, *Phys. Rev. Lett.* **76**, 4620 (1996).
- <sup>6</sup>R. E. Camley and D. Li, *Phys. Rev. Lett.* **84**, 4709 (2000).
- <sup>7</sup>D. Qian, X. F. Jin, J. Barthel, M. Klaua, and J. Kirschner, *Phys. Rev. Lett.* **87**, 227204 (2001).
- <sup>8</sup>A. Biedermann, R. Tscheliessnig, M. Schmid, and P. Varga, *Phys. Rev. Lett.* **87**, 086103 (2001).
- <sup>9</sup>T. Bernhard, M. Baron, M. Gruyters, and H. Winter, *Phys. Rev. Lett.* **95**, 087601 (2005).
- <sup>10</sup>J. Shen, H. Jenniches, Ch. V. Mohan, J. Barthel, M. Klaua, P. Ohresser, and J. Kirschner, *Europhys. Lett.* **43**, 349 (1998).
- <sup>11</sup>H. Jenniches, J. Shen, Ch. V. Mohan, S. S. Manoharan, J. Barthel, P. Ohresser, M. Klaua, and J. Kirschner, *Phys. Rev. B* **59**, 1196 (1999).
- <sup>12</sup>J. Shen, Z. Gai, and J. Kirschner, *Surf. Sci. Rep.* **52**, 163 (2004).
- <sup>13</sup>T. D. Pope, G. W. Anderson, K. Griffiths, P. R. Norton, and G. W. Graham, *Phys. Rev. B* **44**, 11518 (1991).
- <sup>14</sup>H. L. Meyerheim, E. Soyka, and J. Kirschner, *Phys. Rev. B* **74**, 085405 (2006).
- <sup>15</sup>J. Giergiel, J. Kirschner, J. Landgraf, J. Shen, and J. Woltersdorf, *Surf. Sci.* **310**, 1 (1994).
- <sup>16</sup>Y. Shi, J. Zukrowski, M. Przybylski, M. Nyvlt, A. Winkelmann, J. Barthel, and J. Kirschner, *Surf. Sci.* **600**, 4180 (2006).
- <sup>17</sup>M. Zharnikov, A. Dittschar, W. Kuch, C. M. Schneider, and J. Kirschner, *J. Magn. Magn. Mater.* **174**, 40 (1997).
- <sup>18</sup>J. Dorantes-Davila, H. Dreyse, and G. M. Pastor, *Phys. Rev. Lett.* **91**, 197206 (2003).
- <sup>19</sup>M. Weinelt, S. Schwarz, H. Baier, S. Muller, L. Hammer, K. Heinz, and Th. Fauster, *Phys. Rev. B* **63**, 205413 (2001).
- <sup>20</sup>Y. F. Lu, M. Przybylski, M. Nyvlt, A. Winkelmann, L. Yan, Y. Shi, J. Barthel, and J. Kirschner, *Phys. Rev. B* **73**, 035429 (2006).
- <sup>21</sup>D. Qian, X. F. Jin, J. Barthel, M. Klaua, and J. Kirschner, *Phys. Rev. Lett.* **87**, 227204 (2001).
- <sup>22</sup>C. Boeglin, H. Bulou, J. Hommet, X. Le Cann, H. Magnan, P. Le Fevre, and D. Chandessris, *Phys. Rev. B* **60**, 4220 (1999).
- <sup>23</sup>M. Przybylski, L. Yan, J. Zukrowski, M. Nyvlt, Y. Shi, A. Winkelmann, J. Barthel, M. Wasniowska, and J. Kirschner, *Phys. Rev. B* **73**, 085413 (2006).
- <sup>24</sup>Y. Shi, M. Przybylski, J. Barthel, and J. Kirschner (unpublished).
- <sup>25</sup>G. A. T. Allan, *Phys. Rev. B* **1**, 352 (1970).
- <sup>26</sup>K. J. Strandburg, D. W. Hall, C. Liu, and S. D. Bader, *Phys. Rev. B* **46**, 10818 (1992).